



# An efficient Parkinson's disease detection framework: Leveraging time-frequency representation and AlexNet convolutional neural network

Siuly Siuly<sup>a,b,\*</sup>, Smith K. Khare<sup>c</sup>, Enamul Kabir<sup>d</sup>, Muhammad Tariq Sadiq<sup>e</sup>, Hua Wang<sup>a</sup>

<sup>a</sup> Institute for Sustainable Industries & Liveable Cities, Victoria University, Melbourne, Australia

<sup>b</sup> Centre for Health Research, University of Southern Queensland, Toowoomba, Australia

<sup>c</sup> Mærsk Mc-Kinney Møller Institute, Faculty of Engineering, University of Southern Denmark, Denmark

<sup>d</sup> School of Mathematics, Physics and Computing, University of Southern Queensland, Toowoomba, Australia

<sup>e</sup> School of Computer Science and Electronic Engineering, University of Essex, Wivenhoe Park, Colchester, CO4 3SQ, United Kingdom

## ARTICLE INFO

### Keywords:

Parkinson's disease detection  
Electroencephalogram signals  
Time-frequency representation  
Wavelet scattering transform  
AlexNet CNN  
Feature extraction

## ABSTRACT

Parkinson's disease (PD) is a progressive neurodegenerative disorder affecting the quality of life of over 10 million individuals worldwide. Early diagnosis is crucial for timely intervention and better patient outcomes. Electroencephalogram (EEG) signals are commonly used for early PD diagnosis due to their potential in monitoring disease progression. But traditional EEG-based methods lack exploration of brain regions that provide essential information about PD, and their performance falls short for real-time applications. To address these limitations, this study proposes a novel approach using a Time-Frequency Representation (TFR) based AlexNet Convolutional Neural Network (CNN) model to explore EEG channel-based analysis and identify critical brain regions efficiently diagnosing PD from EEG data. The Wavelet Scattering Transform (WST) is employed to capture distinct temporal and spectral characteristics, while AlexNet CNN is utilized to detect complex spatial patterns at different scales, accurately identifying intricate EEG patterns associated with PD. The experiment results on two real-time EEG PD datasets: San Diego dataset and the Iowa dataset demonstrate that frontal and central brain regions, including AF4 and AFz electrodes, contribute significantly to providing more representative features compared to other regions for PD detection. The proposed architecture achieves an impressive accuracy of 99.84% for the San Diego dataset and 95.79% for the Iowa dataset, outperforming existing EEG-based PD detection methods. The findings of this research will assist to create an essential technology for efficient PD diagnosis, enhancing patient care and quality of life.

## 1. Introduction

Parkinson's disease (PD) is a rapidly growing progressive neurodegenerative condition that leads to significant disability and mortality rates. PD stands as the second most common neurodegenerative disorder, following Alzheimer's disease and the most prevalent movement disorder in the world [1]. The condition primarily impacts the central nervous system, particularly the regions of the brain responsible for motor control. PD manifests with a diverse range of motor and non-motor symptoms. The motor symptoms include resting tremors, bradykinesia (slowness of movement), rigidity (muscle stiffness), and postural instability leading to balance issues. Meanwhile, non-motor symptoms can encompass depression, anxiety, sleep disturbances, constipation, and cognitive changes [2,3]. When the disease progresses, the

symptoms become increasingly severe, significantly impacting the daily life and work of patients. The worsening symptoms lead to higher rates of disability and increased need for care [4]. Many people with PD also develop dementia during the course of their disease.

Although the exact causes of PD are not yet entirely known, genetics [5], environment [6], ageing [7], and additional factors like inflammation, oxidative stress, and mitochondrial dysfunction [8] have all been linked to the condition's onset. Age is a significant risk factor, being more frequent in individuals over 60 years old and men are more susceptible to PD than women. According to the Parkinson's Foundation, over 10 million people worldwide are estimated to live with Parkinson's disease, and this prevalence is projected to double by 2040 [4, 9]. As there is currently no cure for Parkinson's disease, and it persists as a lifelong condition, early detection, prompt diagnosis, and appropriate

\* Corresponding author. Institute for Sustainable Industries & Liveable Cities, Victoria University, Melbourne, Australia.

E-mail address: [siuly.siuly@vu.edu.au](mailto:siuly.siuly@vu.edu.au) (S. Siuly).

<https://doi.org/10.1016/j.combiomed.2024.108462>

Received 13 October 2023; Received in revised form 7 April 2024; Accepted 7 April 2024

Available online 9 April 2024

0010-4825/© 2024 The Authors. Published by Elsevier Ltd. This is an open access article under the CC BY license (<http://creativecommons.org/licenses/by/4.0/>).

treatment are vital in enabling affected individuals to lead fulfilling lives. These interventions enable individuals to maintain their regular daily lives to the best extent possible. Therefore, researchers are actively exploring early detection methods to identify vulnerable patients and commence treatment as soon as possible, allowing them to lead as normal a life as possible within society.

There is no definitive test for PD recognition. Diagnosis is typically based on clinical observation of symptoms and a patient's medical history. Neurological examinations and brain imaging techniques, such as Magnetic Resonance Imaging (MRI) and Positron emission tomography (PET) scans, Electroencephalography (EEG) may be used to rule out other possible causes of symptoms [2]. Out of these, EEG holds significant importance in PD diagnosis as it provides a non-invasive means of studying changes in brain activity associated with the condition [3]. This valuable tool allows researchers to gain insights into the underlying mechanisms of Parkinson's disease and explore innovative treatments to improve the quality of life for those affected by the disorder. In individuals with PD, EEG can reveal certain abnormalities in brain wave patterns. These abnormalities are indicative of disrupted brain function and can provide valuable clues about the presence and severity of the disease. Abnormal EEG patterns may also help in tracking the progression of PD over time [2,3].

In the literature, a variety of techniques for the automated diagnosis of PD using EEG signals have been proposed. These methods examined computer-aided diagnostic systems that might automatically distinguish PD patients from healthy controls and learn the EEG characteristics that distinguish PD patients from healthy controls. Li et al. [10] introduced hybrid deep neural networks (DNNs), which construct parallel and series combination models to integrate convolutional neural networks (CNN) with long short-term memory (LSTM). EEG data from 25 patients with PD and 30 healthy controls were used to test the approach and their proposed parallel model achieved 97.6% specificity, 97.1% sensitivity, and 98.6% accuracy. A graph-based aspirin model for automatic PD identification using EEG signals was presented by Baura et al. [11]. The suggested method was evaluated on 16 healthy patients (9 Female, 7 Male), 15 PD (8 Female, 7 Male), and achieved the best classification performance of 95.48%. In order to automatically decompose PD utilizing EEG from 16 healthy controls (HC) and 15 PD (ON and OFF medication) subjects, Khare et al. [12] presented an automated tuneable Q wavelet transform (A-TQWT) by extracting five significant characteristics. The suggested technique correctly classified HC vs PD OFF and HC vs PD ON medications with accuracy rates of 96.13% and 97.65%, respectively.

A random-forest classifier was developed by De Oliveira et al. [13] to offer a machine-learning technique for PD identification that has a classification accuracy of 99.22%. Using EEG data from many research institutes, including healthy subjects and PD patients, Anjum et al. [14] developed a system for identifying PD and achieved 85.40% accuracy. Using 20 healthy cases and 20 PD patients, Balestrino & Schapira [15] proposed a method based on the RUSBoosted trees classifier for PD identification and achieved 87% accuracy. In order to extract high-order features from EEG data for PD identification, Yuvaraj et al. [16] used a machine-learning strategy based on an SVM classifier and attained a classification accuracy of 99.62%. Using a combination of magnetoencephalography and EEG signals, Naghsh et al. [17] developed an automated method for diagnosing PD on 20 participants, 10 of whom had the disease and 10 of whom did not. They reached a 95% accuracy rate. A 13-layer CNN was developed by Oh et al. [18] using resting-state EEG, and it successfully recognized de novo PD with an accuracy of 88.25%. A tuneable Q wavelet transform, and a probabilistic neural network were reported to be used by Murugappan et al. [19] to recognise PD. Wagh et al. [20] proposed an 8-layer graph-CNN that could identify PD and other neurological conditions with an accuracy of 85%.

For the purpose of PD identification, Xu et al. [21] developed a pooling based deep RNN technique and reported, in that order, 91.81% specificity, 84.84% sensitivity, and 88.31% accuracy. With an area

under the curve (AUC) of 91%, Koch et al. [22] developed a Random Forest Classifier for PD detection using clinical and automated characteristics from EEG data. Two hybrid models for diagnosing PD were introduced by Shi et al. [23] with the highest accuracy of 82.89%. With 96.9% accuracy. Lee et al. [24] developed a hybrid model combining CNN and LSTM to take advantage of the spatial and temporal characteristics of EEG. Discrete wavelets transform (DWT)-based approach [3], smoothed pseudo-Wigner Ville distribution (SPWVD) coupled with CNN based approach [6], deep-learning approach based on layer convolutional neural network [1] are some additional techniques that use PD detection using EEG. Several popular deep learning models have been introduced in Refs. [25–29] to enhance performance, stability, and decrease false discovery rate.

The existing literature highlights certain gaps in the current methods for PD identification using EEG signals. Notably, the combination of time-frequency representation (TFR) with deep learning models, which is crucial for efficiently identifying PD, has not been extensively explored. EEG signals exhibit complexity and diversity, being non-periodic, non-stationary, and non-linear, making TFR and deep learning integration highly relevant. Additionally, the current research has overlooked the investigation of the individual contributions of different EEG channels and the specific brain regions responsible for detecting PD as potential biomarkers. Understanding the involvement of specific brain regions could aid in refining diagnostic accuracy. Furthermore, many studies in the field of EEG-based PD detection are based on relatively small sample sizes and may lack external validation on larger and more diverse datasets. In summary, the current literature indicates the need for further research to address these limitations by exploring TFR in combination with deep learning models, investigating EEG channel contributions and brain region involvement, and validating findings on more extensive and diverse datasets for enhanced PD detection and diagnostic accuracy.

To address the existing issues, this study intends to design a Time-Frequency Representation (TFR) based AlexNet network model for PD detection using EEG signals with the aim of achieving the following three objectives: (1) Develop a computationally efficient and straightforward model for PD classification using EEG; (2) Investigate the effect of different EEG channels in PD detection to localize the brain region responsible for selecting representative channels; (3) Enhance the performance of the proposed model compared to state-of-the-art methods. For the first time, this study is to introduce the Wavelet Scattering Transform (WST), a method tailored to handle the oscillatory nature of EEG signals effectively, in conjunction with the AlexNet model for accurate PD detection. In the proposed framework, WST is used to present TFR for handling the oscillatory nature of EEG signals more precisely. Additionally, the AlexNet model is utilized effectively in detecting PD leveraging the TFR information obtained from EEG data.

The proposed approach offers significant contributions, which can be summarized as follows:

- We have designed a new framework for PD detection, integrating TFR and AlexNet AlexNet-CNN algorithms. This framework efficiently distinguishes between healthy control and PD subjects using real-time EEG datasets. Notably, we are the first to employ the WST-based TFR in combination with AlexNet-CNN, and our approach has been successfully tested on these two datasets.
- Through our research, we have conducted a thorough channel-wise analysis of EEG data, leading to the localization of the brain region responsible for selecting the representative channel. This investigation provides valuable insights into the neural mechanisms underlying PD detection through EEG signals.
- We investigated the effectiveness of the AlexNet model by comparing it with three widely used CNN models, VGG16, DarkNet19 and ResNet18, within the proposed framework to establish a robust PD detection scheme.

- The proposed AlexNet based approach exhibits superior performance in PD detection from EEG data compared to existing state-of-the-art EEG-based PD detection methods. The model's improved accuracy and efficacy represent a significant advancement in the field of EEG-based PD diagnosis.

The structure of this paper is outlined as follows: Section 2 offers a comprehensive account of the EEG datasets utilized in this study and an overview of the proposed PD detection framework. In Section 3, detailed information about the experimental setup, experimental results, and corresponding discussions is presented. Section 4 presents a discussion about the study and its findings. Lastly, Section 5 concludes the paper and includes insights into future research directions.

## 2. Material and methods

### 2.1. Datasets

**Dataset 1 (Iowa dataset):** This dataset was obtained from studies conducted at the University of Iowa (UI) in Iowa City, Iowa [14,30]. This dataset consists of EEG recordings from 14 individuals with PD and 14 healthy control (HC) subjects. The participants were not subjected to any exclusion criteria. However, the HC participants were carefully matched with PD patients in terms of age and sex, and no significant differences were observed in education or premorbid intelligence (Table 1). During the experimental protocol, EEG recordings in the Iowa dataset were obtained only under eyes-open conditions. The EEG data were captured using 0.1–100 Hz sintered Ag/AgCl electrodes on a 64-channel Brain Vision system. The sampling rate used was 500 Hz, and each subject's EEG was recorded for at least 2 min. An online reference was set to channel Pz as the baseline. Further details about these datasets can be found in Ref. [14].

**Dataset 2 (San Diego dataset):** Dataset 2 is an openly accessible dataset collected at the University of San Diego, California [31]. This dataset comprises data from 16 healthy control participants (7 males and 9 females) with an average age of  $63.5 \pm 9.6$  years, and 15 individuals diagnosed with PD (8 females and 7 males) with an average age of  $63.2 \pm 8.2$  years. The PD patients were carefully matched to the healthy control group in terms of right-handedness, gender, age, and cognitive abilities, as assessed by the Mini-Mental State Exam and North American Adult Reading Test. All PD patients in the dataset had mild to moderate disease (Stage II and III on the Hoehn and Yahr scale), with an average disease duration of  $4.5 \pm 3.5$  years. The data collection involved recordings on different days, with a counterbalanced order for PD patients with medication ON (PDSO) and OFF (PDSF) conditions. For PDSO recordings, the subjects maintained their normal medication schedule, while for PDSF recordings, the patients refrained from taking medication for at least 12 h. Healthy control subjects were tested only once. During data collection, the subjects were seated comfortably and asked to relax while fixating their eyes on a cross displayed on a screen. EEG data were recorded for a minimum of 3 min using a 32-channel Biosemi ActiveTwo EEG system at a sampling frequency of 512 Hz. For a more detailed description of the dataset, data acquisition, and

**Table 1**  
Demographic information of PD and healthy participants.

Category	Dataset 1: Iowa dataset		Dataset 2: San Diego dataset	
	HC	PD	HC	PD
Number of Participants	14	14	16	15
Gender (Male/female)	6/8	6/8	7/9	8/7
Age (years)	$70.5 \pm 8.7$	$70.5 \pm 8.7$	$63.5 \pm 9.6$	$63.2 \pm 8.2$
Disease duration (years)	–	$5.6 \pm 3.2$	–	$4.5 \pm 3.5$
Sampling Frequency (Hz)	500	500	512	512
Used number of channel	64	64	32	32

pre-processing, please refer to Refs. [3,31,32].

### 2.2. Proposed methodology

In this study, a novel framework is presented for identifying PD from EEG data, which involves a combination of Wavelet Scattering Transform (WST) and AlexNet-based Convolutional Neural Network (CNN) model. The WST is used to obtain Time frequency representation (TFR) of EEG signal data. The proposed method comprises several essential steps, including pre-processing, time-frequency representation, hidden feature extraction, and classification. Fig. 1 visually demonstrates the design concept of the proposed framework in this research. Detailed explanations of each phase within the proposed framework are provided in the following sections.

#### 2.2.1. Phase 1: time frequency representation using wavelet scattering transform (WST)

Time-frequency representation (TFR) is a valuable method for analyzing EEG signals, as it allows for simultaneous examination of both the time and frequency domains. This capability is essential in detecting PD because the disease exhibits distinct temporal and spectral characteristics that may not be readily discernible when studying each domain independently. In this research, the Wavelet Scattering Transform (WST) tool is employed to obtain the TFR of EEG signals, which effectively captures both local and global structures within the data. By leveraging TFR, we can better capture and identify the unique patterns associated with PD, enhancing our ability to diagnose and understand the condition.

The WST builds upon the principles of wavelet analysis belonging to the family of wavelet transforms and operates on scattering coefficients derived from wavelet transforms, modulus nonlinearities, and averaging. It involves iteratively applying wavelet transforms to a signal at various scales, computing the modulus of the resulting coefficients at each scale, and then recombining them to create a new representation of the signal [33]. This resultant representation offers insights into the signal's structure at different scales, making it advantageous for analyzing signals with multi-scale characteristics. This transform is particularly valuable when examining signals exhibiting intricate and multi-scale structures, as it enables the extraction of information at multiple scales and resolutions.

Instead of traditional WT, this study considers WST for EEG-based PD detection for these reasons: (1) Better Time-Frequency Representation: It provides a more accurate representation of EEG signals, capturing high and low-frequency components effectively, crucial for identifying relevant patterns in PD-related EEG data. (2) Multiscale Analysis: It performs hierarchical decomposition across multiple scales, enabling detection of subtle changes and abnormalities in EEG data associated with PD. (3) Reduced Computational Complexity: Compared to traditional WT, WST has lower computational complexity, making it more efficient for processing large EEG datasets common in PD detection studies.

The stages involved in the WST for generating scattering coefficients are visually depicted in Fig. 2. Fig. 3 presents a tree overview diagram illustrating the zero-order scattering coefficients obtained through averaging. In Fig. 3,  $f$  represents the input EEG signal,  $\varphi_J$  is the scaling function, and  $\{\psi_{j,k}\}$  are the wavelets, respectively. The features are iteratively generated by wavelet scattering transform. Firstly, input EEG data is convolved with scaling function ( $f^* \varphi_J$ ) to generate the zeroth-order scattering coefficients,  $S[0]$ . As a next step, following process is repeated for each node [34].

- Perform the WT of EEG data with each wavelet filter in the first filter bank.
- Next, the modulus of each filtered output should be calculated. The nodes are the scalogram,  $U$  [1].

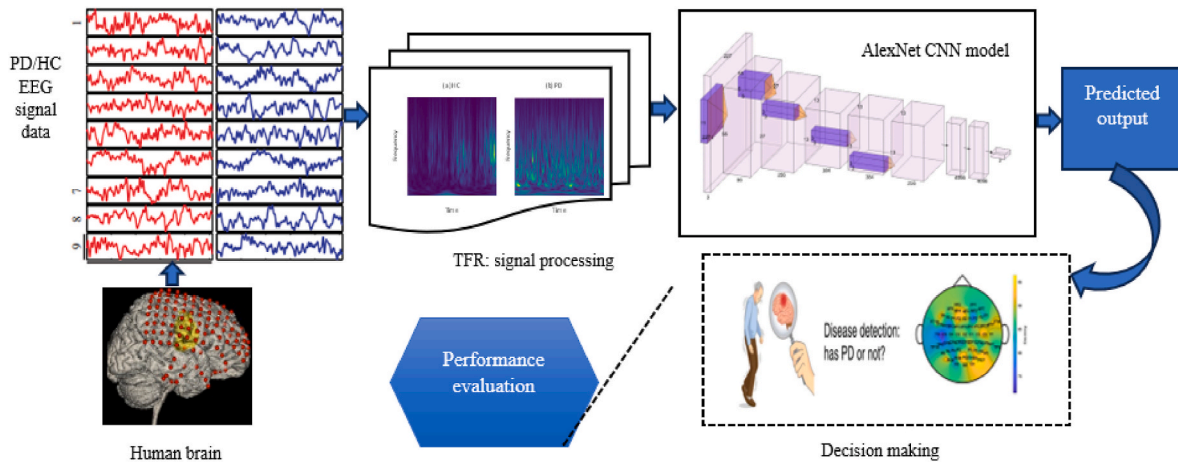


Fig. 1. Overall framework of our proposed model for efficient identification of PD using EEG data.

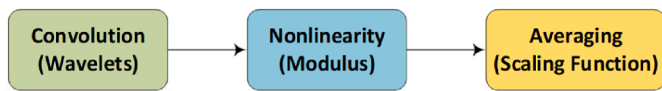


Fig. 2. Stages involved in scattering wavelet transform.

- Utilizing the scaling filter, average each modulus. The outcomes are the first-order scattering coefficients,  $S [1]$ .

The details descriptions of WST are available in Refs. [33,34]. The WST based TFR allows for the extraction of time-varying frequency information from EEG signals, enabling the detection of subtle changes and patterns associated with PD.

Figs. 4 and 5 display the TFR acquired through the use of WST on Dataset 1 and Dataset 2, respectively. By observing these figures, it

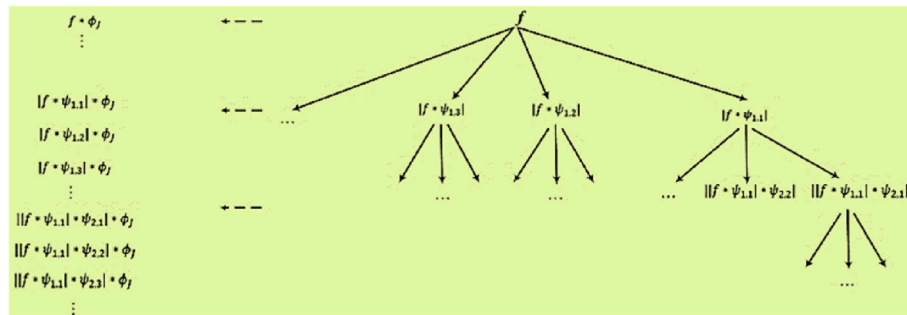


Fig. 3. Tree view of zeroth-order scattering coefficients computed by simple averaging of the input (<https://au.mathworks.com/help/wavelet/ug/wavelet-scattering.html>).

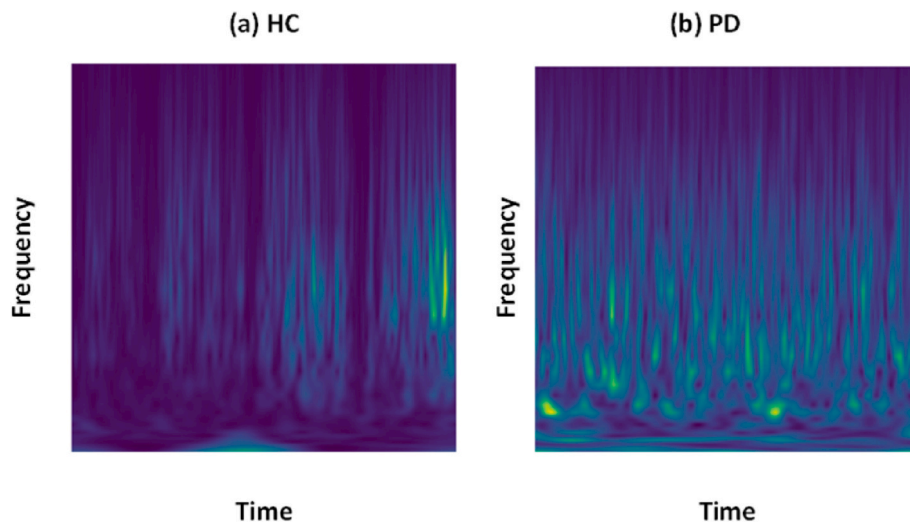


Fig. 4. Exemplary TFR obtained using WST on Dataset 1 (a) HC and (b) PD.



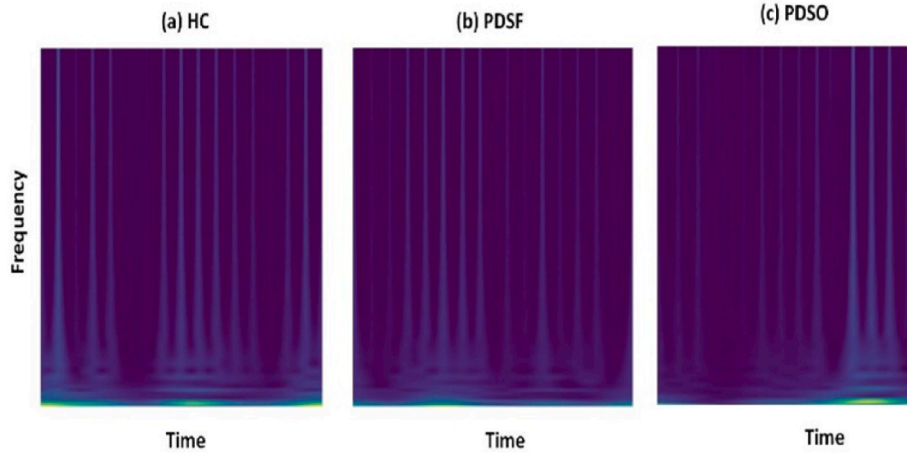


Fig. 5. Exemplary TFR obtained using WST on Dataset 2 (a) HC, (b) PDSF, and (c) PDSO.

becomes apparent that the TFR of healthy controls (HC) and individuals with PD on Dataset 1 exhibit distinct features. Similarly, the TFR of HC, individuals with PD in the “on” state (PDSF), and individuals with PD in the “off” state (PDSO) on Dataset 2 also exhibit representative characteristics. These findings highlight the ability of TFR to capture intricate details of EEG signals during PD, enabling the generation of distinguishable patterns for differentiating between HC and PD EEG signals.

2.2.2. Phase 2: model architecture: AlexNet based CNN model

Automated PD detection relies heavily on effective decision-making. In this study, we propose an architecture for extracting important hidden features from EEG data for PD detection that involves a TFR-based AlexNet CNN model. The main motivation behind choosing the AlexNet-based CNN model for EEG-based PD detection lies in its simplicity and proficiency in capturing complex spatial patterns within the EEG data. Specific features of AlexNet, such as its deep architecture and convolutional layers, make it well-suited for extracting hierarchical features from EEG signals. Further details outlining the reasons are provided as follows: (1) AlexNet presents a deeper architecture compared to other CNN models, facilitating the capture of more intricate features within the data. This increased depth empowers the model to acquire hierarchical representations, essential for comprehending the complex patterns inherent in EEG signals associated with PD. (2) AlexNet incorporates local response normalization, a technique enhancing the model’s generalization by normalizing responses across various channels. This normalization mechanism enhances the model’s robustness to variations and assists in capturing pertinent patterns within the EEG signals. (3) The convolutional filters utilized in AlexNet are constructed to identify spatial patterns at diverse scales. This characteristic proves advantageous for capturing both local and global patterns within EEG signals, a crucial aspect for precise identification of PD-related abnormalities.

AlexNet is a pioneering convolutional neural network architecture. It consists of eight layers, including five convolutional layers, and three fully connected layers. The initial five layers are convolutional, and in

some cases, they are followed by max-pooling layers. The remaining three layers were fully connected. To facilitate parallel processing, the network is split into two copies, with each copy running on one GPU [35]. The overall can be summarized as follows in Fig. 6:

The five convolutional layers of the AlexNet CNN model are used to extract the input image’s deep information [35,36]. The number and size of the filters in the convolutional layer varies. For the study of deep features, the filter is moved around as a tensor or an image. The subsequent input receives the extracted deep features and continues the extraction of deep features there. Three completely connected layers that reduce the two-dimensional feature matrix to one dimension form the CNN model’s final layer. Softmax layer, which allocates the class based on a probabilistic approach, is used to end the model. Fig. 7 depicts the AlexNet model’s schematic structure. Table 2 provides an overview of the CNN model’s tuning parameters for this proposed model.

2.2.3. Phase 3: predicted outcome and decision-making

In this phase, predicted outcomes (e.g., PD or HC classification) are obtained through two fully connected layers, which constitute the final layer of the AlexNet CNN model and produce a probability distribution

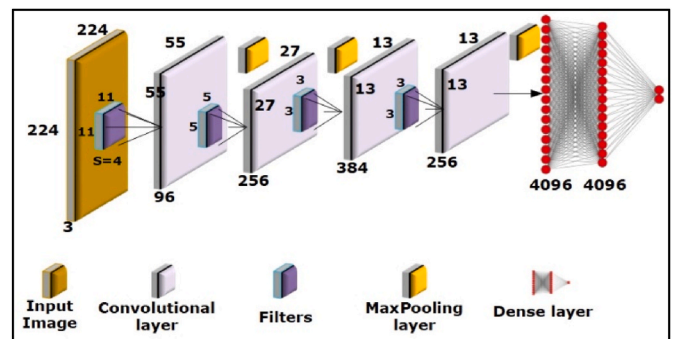


Fig. 7. Schematic diagram of AlexNet CNN model.



Fig. 6. Working steps of AlexNet model.

Where, CNN = convolutional layer (with ReLU activation); RN = local response normalization; MP = maxpooling; FC = fully connected layer (with ReLU activation); Linear = fully connected layer (without activation); DO = dropout.

**Table 2**  
Summary of the tuning parameters of the proposed Alexnet model.

Name	No. of filters/ neurons	Size of filter	Stride	Padding	Size of feature maps	Activation	Weights	Biases	No. of learnable parameters
Input	–	–	–	–	227 × 227 × 3	–	–	–	–
Convolution Layer 1	96	11 × 11	4	–	55 × 55 × 96	ReLU	34848	96	34944
MaxPooling 1	–	3 × 3	2	–	27 × 27 × 96	–	0	0	0
Convolution Layer 2	256	5 × 5	1	2	27 × 27 × 256	ReLU	614400	256	614656
MaxPooling 2	–	3 × 3	2	–	13 × 13 × 256	–	0	0	0
Convolution Layer 3	384	3 × 3	1	1	13 × 13 × 384	ReLU	884736	384	885120
Convolution Layer 4	384	3 × 3	1	1	13 × 13 × 384	ReLU	1327104	384	1327488
Convolution Layer 5	256	3 × 3	1	1	13 × 13 × 256	ReLU	884736	256	884992
MaxPooling 3	–	3 × 3	2	–	6 × 6 × 256	–	0	0	0
Dropout 1	Rate = 0.5	–	–	–	6 × 6 × 256	–	0	0	0
Fully connected layer 1	–	–	–	–	4096	ReLU	37748736	7096	37752832
Dropout 2	Rate = 0.5	–	–	–	4096	–	0	0	0
Fully connected layer 2	–	–	–	–	4096	ReLU	16777216	4096	16781312
Fully connected layer 3	–	–	–	–	2	ReLU	8192	2	8194
Total learnable parameters	58289538	–	–	–	–	–	–	–	–

over all possible categories for the given input (refer to Fig. 6). The final layer employs a softmax function, yielding output probabilities ranging from 0 to 1 for each class in the classification task. These output probabilities represent the predicted likelihood of the input signal belonging to a specific class, where higher probabilities indicate greater confidence in the classification. Ultimately, based on these probabilities, decisions are made regarding the number of subjects classified as PD and the number classified as HC.

#### 2.2.4. Phase 4: performance evaluation

The consistency of a decision-making model is determined by its overall performance. In the context of a medical expert decision-making system, multiple evaluations are conducted to assess the system comprehensively. To gauge the overall consistency of our developed model, we have assessed four performance measures in addition to accuracy. These measures include sensitivity (SEN), specificity (SPE), precision (PPV), and F-1 score. The mathematical expressions for these performance measures are defined as follows:

$$\text{Accuracy} = \frac{P_t + N_t}{P_t + P_f + N_t + N_f}; \text{ Sensitivity} = \frac{P_t}{P_t + N_f};$$

$$\text{Specificity} = \frac{N_t}{P_f + N_t}; \text{ Precision} = \frac{P_t}{P_t + P_f}$$

$$F - 1 \text{ score} = \frac{2 * \text{Precision} * \text{Sensitivity}}{\text{Precision} + \text{Sensitivity}}$$

where  $P_t$ ,  $P_f$ ,  $N_t$ , and  $N_f$  are true positive, false positive, true negative, and false negative values.

### 3. Results

This study assessed the proposed TFR-based AlexNet CNN model using two real-time PD EEG datasets: the Iowa dataset (dataset 1) and the San Diego dataset (dataset 2). In this section, firstly we present a brief overview of the experimental setup for the model implementation. Subsequently, we present the results obtained from the experiments. Finally, we provide a comparative analysis with existing methods in the field, followed by a discussion of the findings.

#### 3.1. Experimental set up

The analysis of EEG signals poses challenges due to their non-stationary nature. Despite its excellent temporal resolution, EEG suffers from limited spatial resolution. To address this limitation, many electrodes are used for analysis, but this raises the issue of determining

the most effective electrodes for the task. Previous works have typically explored the analysis of all channels, making it difficult to localize specific brain regions accurately. In this study, we propose a novel approach that focuses on individual channel analysis to improve brain region localization. Our methodology involves using the WST for time-frequency analysis, allowing us to extract simultaneous information about time and frequency characteristics. These time-frequency characteristics obtained from the WST are fed into the AlexNet CNN model, which facilitates automatic extraction and classification of deep features. To ensure effective analysis, we maintain a common experimental setup.

For the WST, we set the quality factor to Refs. [1,2,4]. In this study, the CNN models are evaluated using train-test split validation on the dataset, where the data is divided into training and testing sets to assess the model. We allocated 80% of the data for training, and the remaining portion designated for testing or validation. To mitigate overfitting and potential bias, we validated the model several times using ‘holdout validation’ technique. In this method, the dataset is randomly partitioned into training and validation (or test) sets. The training set is utilized for model training, while the validation set (or test set) is reserved for evaluating its performance. This holdout validation process, involving random splits into train-test sets, is performed iteratively to enhance robustness against overfitting and bias. The model undergoes five iterations with random splits, and the final results are obtained by averaging the testing accuracy across the five holdout validations. To fine-tune the CNN model, we set the bias and weight learn factors to 20, use a batch size of 16, and employ a learning rate of 1e-4. The maximum epoch size is set to 15 to ensure optimal training. Through this approach, we aim to overcome the challenges posed by EEG’s non-stationary nature and limited spatial resolution while improving the accuracy of brain region localization.

#### 3.2. Experimental results

PD is a complex neurological disorder, and its detection requires a comprehensive analysis of multiple brain regions and their EEG signals. Table 3 presents the channel-wise accuracy achieved on dataset 1 (Iowa dataset) for detecting PD vs HC. Fig. 8 provides a comprehensive view of the variations in channel-wise performance across each channel on dataset 1. The findings reveal that channel AFz attained the highest accuracy of 95.79%. Additionally, our developed model successfully generated representative features in ‘Anterior Frontal midline regions’ (situated on the midline of the forehead), while the parietal region also exhibited significant deep features, contributing to its higher accuracies.

As mentioned before, Dataset 2 (San Diego dataset) consists of three conditions: PD patients with ON (PDSO) and OFF medication (PDSF), as

**Table 3**  
Channel-Wise Accuracy (%) Achieved with the Proposed Model For HC vs PD On Dataset 1.

Channel	Channel Name	Overall accuracy	Channel	Channel Name	Overall accuracy
1	'Fp1'	88.89	33	'AF3'	89.67
2	'Fz'	90.42	34	'AFz'	<b>95.79</b>
3	'F3'	86.21	35	'F1'	92.72
4	'F7'	91.57	36	'F5'	85.44
5	'FT9'	84.29	37	'FT7'	88.51
6	'FC5'	86.21	38	'FC3'	77.01
7	'FC1'	88.89	39	'C1'	86.97
8	'C3'	84.67	40	'C5'	71.26
9	'T7'	78.93	41	'TP7'	83.52
10	'TP9'	82.38	42	'CP3'	83.14
11	'CP5'	75.86	43	'P1'	85.06
12	'CP1'	85.44	44	'P5'	86.59
13	'P3'	81.61	45	'PO7'	92.34
14	'P7'	85.44	46	'PO3'	81.99
15	'O1'	82.38	47	'POz'	93.49
16	'Oz'	87.74	48	'PO4'	85.06
17	'O2'	91.57	49	'PO8'	95.48
18	'P4'	92.72	50	'P6'	86.59
19	'P8'	91.95	51	'P2'	88.12
20	'TP10'	84.67	52	'CPz'	82.76
21	'CP6'	84.67	53	'CP4'	86.59
22	'CP2'	90.42	54	'TP8'	89.27
23	'Cz'	89.66	55	'C6'	93.10
24	'C4'	86.97	56	'C2'	86.59
25	'T8'	89.66	57	'FC4'	89.66
26	'FT10'	91.19	58	'FT8'	89.66
27	'FC6'	89.27	59	'F6'	89.27
28	'FC2'	85.82	60	'AF8'	85.44
29	'F4'	76.25	61	'AF4'	84.67
30	'F8'	83.14	62	'F2'	89.66
31	'Fp2'	85.06	63	'FCz'	86.97
32	'AF7'	87.36			

**Table 4**  
Channel-Wise Accuracy (In Percentage) Achieved with the Proposed Model For HC vs PDSF And HC vs PDSO On Dataset 2.

Channel	Channel Name	Overall accuracy	Channel	Channel Name	Overall accuracy
1	'Fp1'	96.53	1	'Fp1'	97.52
2	'AF3'	92.73	2	'AF3'	94.22
3	'F7'	97.85	3	'F7'	98.18
4	'F3'	99.00	4	'F3'	98.84
5	'FC1'	94.71	5	'FC1'	97.85
6	'FC5'	97.85	6	'FC5'	96.53
7	'T7'	91.74	7	'T7'	94.71
8	'C3'	93.72	8	'C3'	95.54
9	'CP1'	94.22	9	'CP1'	97.52
10	'CP5'	98.18	10	'CP5'	96.86
11	'P7'	93.39	11	'P7'	97.19
12	'P3'	93.39	12	'P3'	98.84
13	'Pz'	94.71	13	'Pz'	98.18
14	'PO3'	90.09	14	'PO3'	97.52
15	'O1'	91.08	15	'O1'	95.58
16	'Oz'	92.24	16	'Oz'	96.86
17	'O2'	92.24	17	'O2'	97.02
18	'PO4'	98.01	18	'PO4'	99.17
19	'P4'	98.18	19	'P4'	97.52
20	'P8'	98.18	20	'P8'	99.00
21	'CP6'	96.53	21	'CP6'	97.02
22	'CP2'	95.54	22	'CP2'	95.54
23	'C4'	99.17	23	'C4'	97.85
24	'T8'	95.54	24	'T8'	97.19
25	'FC6'	97.85	25	'FC6'	98.18
26	'FC2'	98.84	26	'FC2'	99.00
27	'F4'	99.17	27	'F4'	99.17
28	'F8'	97.52	28	'F8'	99.84
29	'AF4'	<b>99.84</b>	29	'AF4'	<b>99.84</b>
30	'Fp2'	97.85	30	'Fp2'	99.00
31	'Fz'	98.18	31	'Fz'	99.17
32	'Cz'	97.85	32	'Cz'	99.17

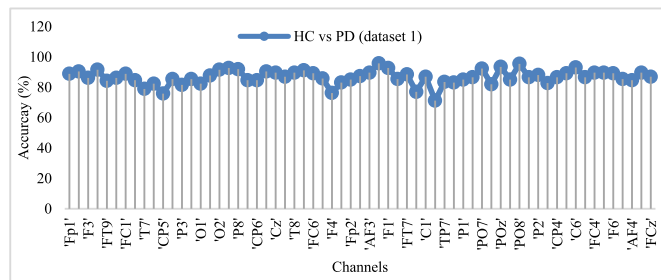


Fig. 8. Visualization of channel-wise performance for dataset 1.

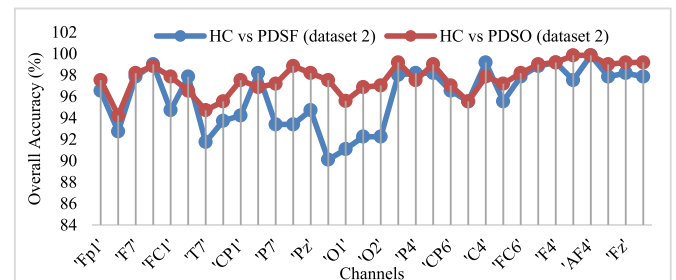


Fig. 9. Visualization of channel-wise performance for dataset 2.

well as HC subjects. We conducted channel-wise accuracy analysis for PDSO vs HC and PDSF vs HC. The accuracy results for individual channels in HC vs PDSF and HC vs PDSO on Dataset 2 are presented in Table 4. Fig. 9 provides a visual representation of the varying performances of each channel. Our analysis reveals that our developed model achieved the highest classification accuracy of 99.84% for channel AF4 in both HC vs PDSO and HC vs PDSF comparisons. AF4 denotes the “Anterior Frontal-right” location which is located on the right side of the forehead, adjacent to AFz. It is important to note that both datasets demonstrate that channel locations in the central and frontal regions (e.g. AF4 and AFz) exhibit more representative features when compared to other regions. Furthermore, the results demonstrate the effectiveness of our developed technique in tracking changes during ON and OFF medication phases of PD patients compared to HC subjects.

In order to gain deeper insights into the brain regions most responsible for PD detection and the generation of representative characteristics, we generated topographic maps for both datasets. These maps play a significant role in understanding PD by providing valuable insights into the spatial distribution of brain activity. Referred to as scalp maps

or voltage maps, they visualize the electrical activity recorded by an EEG or other brain imaging techniques across different regions of the scalp. Fig. 10 displays the topographic map obtained from dataset 1.

Similarly, Figs. 11 and 12 show the topographic maps of accuracy on Dataset 2 for HC vs PDSF and HC vs PDSO, respectively. These figures reveal that in the detection of PD, frontal and central regions play a crucial role in generating the representative characteristics of TFR. Thus, utilizing the topographic maps obtained from accuracy, we have effectively demonstrated the role of various brain regions in PD detection. Finally, we have plotted the topographic maps obtained on our developed model to determine which portion of the brain has generated representative characteristics for PD detection.

To achieve intense understandings into our developed model, we assessed its performance using four key metrics. Table 5 presents the performance parameters obtained for

Dataset 1 and dataset 2 using our proposed model. The analysis indicates that on Dataset 1, the model achieved a sensitivity (SEN) of 96.09%, specificity (SPE) of 95.49%, positive predictive value (PPV) of 95.35%, and F1 score of 95.42%. On Dataset 2, for the classification of

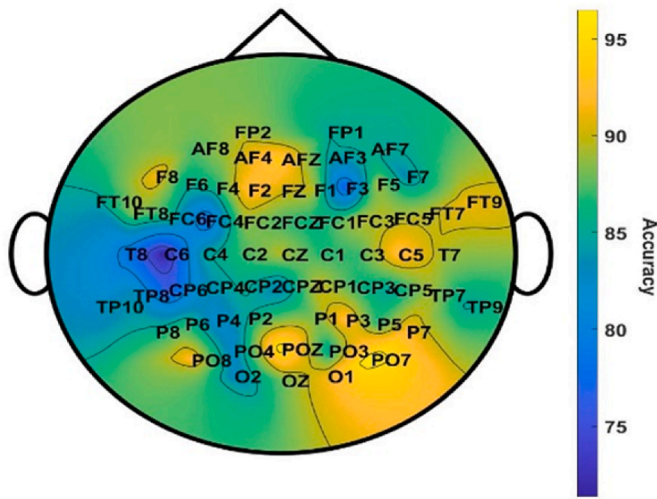


Fig. 10. Topographic map of HC vs PD obtained for dataset 1.

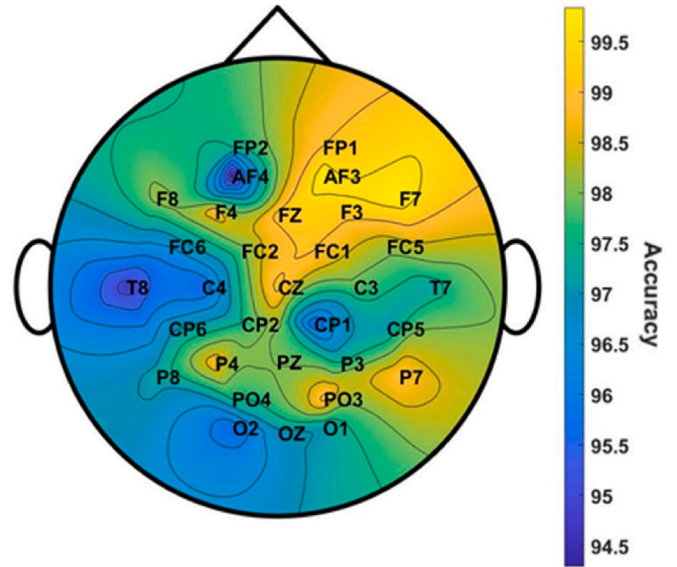


Fig. 12. Topographic map of HC vs PDSO obtained for dataset 2.

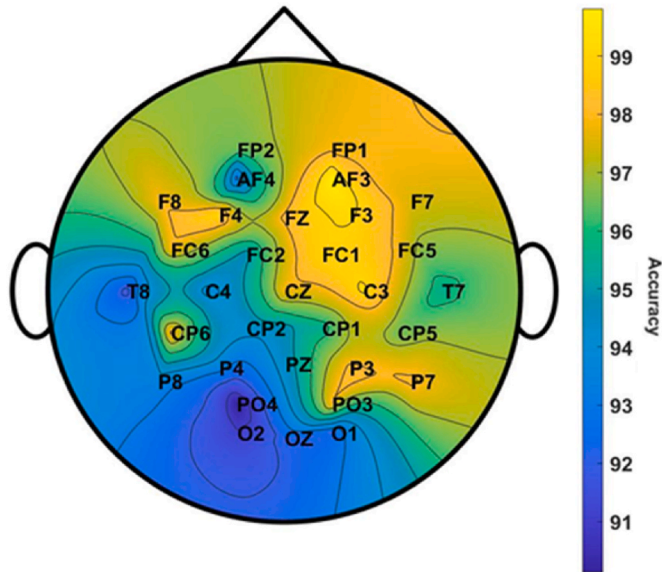


Fig. 11. Topographic map of HC vs PDSF obtained for dataset 2.

PDSF vs HC, our model achieved an SEN of 100%, SPE of 99.67%, PPV of 100%, and F1 score of 99.84%. Meanwhile, for the classification of PDSO vs HC, our model obtained an SPE of 100%, SEN of 99.67%, PPV of 99.67%, and F1 score of 99.84%. These results demonstrate the consistency and effectiveness of our developed model in accurately detecting PD and HC EEG signals.

In order to determine the individual detection rates of HC and PD for two datasets, we computed the confusion matrix. The results are presented in Table 6, showing the percentage accuracy obtained for HC and PD classification on dataset 1.

Our model achieved an accuracy of 95.35% for PD detection and 96.21% for HC detection. Similarly, in the classification of PDSF, PDSO, and HC on dataset 2, the confusion matrix results are displayed in Table 7. The model demonstrated 100% accuracy in detecting HC and PDSO, while achieving an accuracy of 99.67% for PDSF detection. These findings highlight the effectiveness of our developed model in accurately classifying PD and HC subjects in both datasets.

Furthermore, we also assessed the performance of our proposed model based on receiver operating characteristics (ROC) as it is a crucial tool in the disease detection and diagnosis. It is widely used to assess the

Table 5  
Performance parameters (percentage) of dataset 1 and dataset 2 using our proposed AlexNet model.

Performance Parameters	HC vs PDSO (dataset 2)	HC vs PDSF (dataset 2)	HC vs PD (dataset 1)
Accuracy	99.83	99.83	95.79
Specificity	100.00	99.67	95.49
Sensitivity	99.67	100.00	96.09
Precision	99.67	100.00	95.35
F1-score	99.84	99.84	95.42

Table 6  
Percentage Confusion Matrix for HC vs PD On Dataset 1.

	HC	PD
HC	96.21	3.79
PD	4.65	95.35

Table 7  
Percentage Confusion Matrix for HC vs PDSF And HC vs PDSO On Dataset 2.

	HC	PDSO
HC	99.67	0.33
PDSO	0	100

	PDSF	HC
PDSF	99.67	0.33
HC	0	100

performance of a binary classification model, such as those used for distinguishing between PD and healthy control subjects. The ROC and area under the curve (AUC) for our developed model on Dataset 1 is shown in Fig. 13. As evident from the Figure, our developed model has



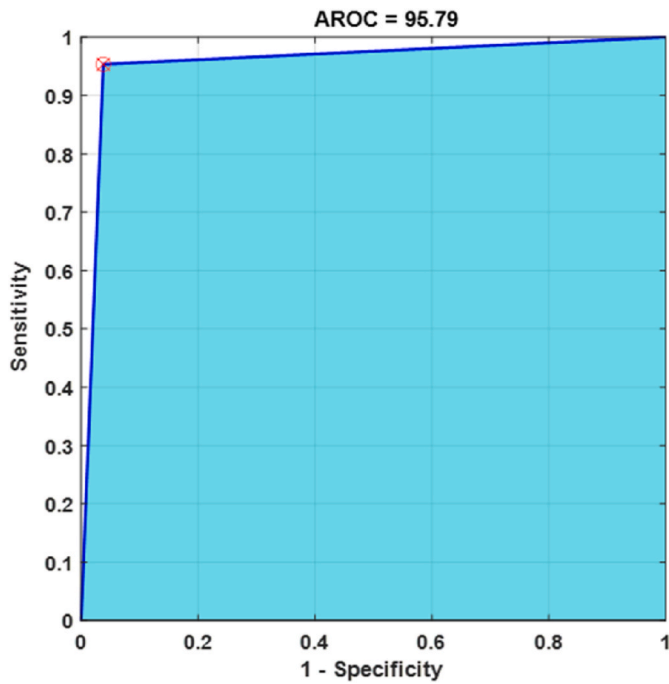


Fig. 13. ROC and AUC obtained for HC vs PD classification on Dataset 1.

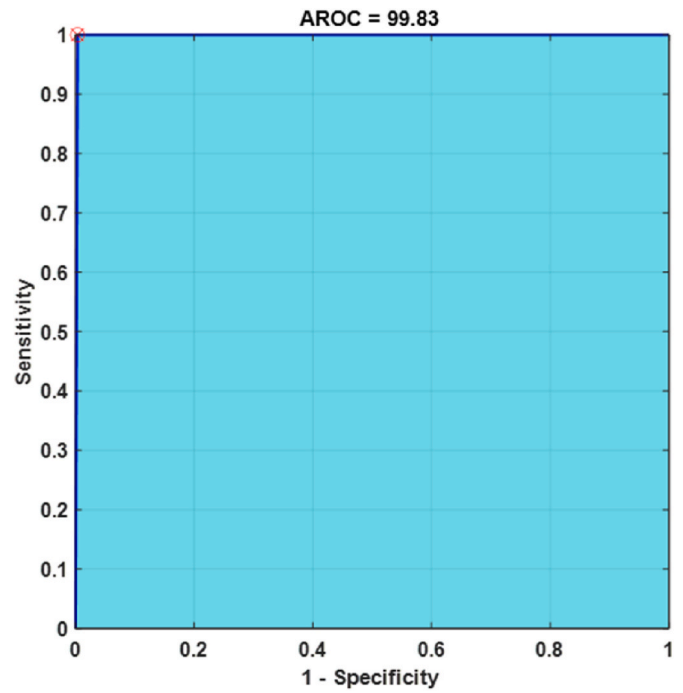


Fig. 15. ROC and AUC obtained for HC vs PDSO classification on Dataset 2.

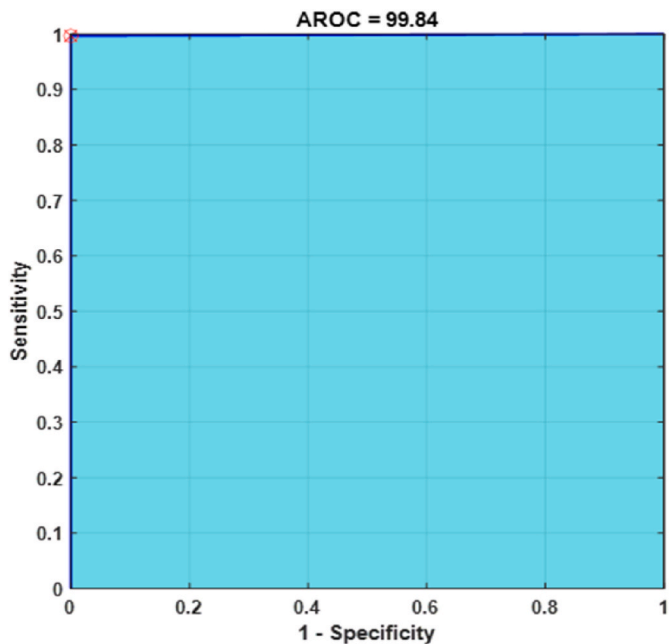


Fig. 14. ROC and AUC obtained for HC vs PDSF classification on Dataset 2.

obtained the AUC of 97.02%. Similarly, the AUC and ROC obtained on dataset2 for HC vs PDSF and HC vs PDSO is shown in Figs. 14 and 15. The figures reveal that our model has achieved the AUC of 100%, denoting ideal performance on dataset 2. Thus, the ROC and AUC analysis shows that our model is highly consistent and accurate in binary classification scenarios.

#### 4. Discussions

This study sought to introduce an innovative hybrid framework that combines a Time-Frequency Representation with a CNN based deep learning model to automate the detection of PD from EEG signals. The

WST was employed to capture distinctive temporal and spectral characteristics, while the AlexNet CNN recognized complex spatial patterns across various scales in the proposed framework. This integration facilitated the precise identification of intricate EEG patterns associated with PD, with the primary goal of developing a framework that effectively differentiates between patients with PD and HC subjects using EEG signal data. The framework also aims to distinguish individuals with PD (off medication) and those with PD (on medication) from HC subjects. The study conducted an investigation to pinpoint the most influential EEG channels and brain regions providing significant information for the effective identification of PD patients. The research includes a multi-pattern analysis, encompassing channel-wise performance examination and brain region investigation through topographic maps, achieving high performance in the effective identification of PD patients through comparative analysis. To assess the framework's effectiveness, tests were conducted on two publicly available datasets: the Iowa dataset (Dataset 1) and the UC San Diego dataset (Dataset 2).

The research findings indicated that the AlexNet-based CNN model achieved its highest accuracy of 95.79%, specifically for channel AFz in dataset 1, surpassing all existing methods. The model exhibited a sensitivity of 96.09%, specificity of 95.49%, positive predictive value (PPV) of 95.35%, and an F1 score of 95.42% for the dataset 1. In dataset 2, the proposed model demonstrated the highest classification accuracy of 99.84% for channel AF4 in both HC vs PDSO and HC vs PDSF. In dataset 2, the model displayed a sensitivity of 100%, specificity of 99.67%, PPV of 100%, and an F1 score of 99.84% when classifying PDSO vs HC. Across both datasets, the study revealed that channels located in the central and frontal regions, such as AF4 and AFz, showcased more representative features compared to other regions. Consequently, the results suggest that future research may not require the use of whole brain EEG channel data for identifying PD; focusing on central and frontal regions should suffice for PD detection. Additionally, the developed model's performance was assessed through ROC, demonstrating high consistency and accuracy in binary classification scenarios, with an AUC of 100% for UC San Diego and an AUC of 97.02% for the Iowa dataset.

To ensure consistency and reliability, a comparison was conducted

between the AlexNet-based CNN model and three other popular CNN models, VGG16, DarkNet19 and ResNet18, within the proposed PD detection framework. Like the AlexNet model, other three models: VGG16, DarkNet19 and ResNet18 also utilized the best performing channels such as AFz for dataset 1 and AF4 for dataset 2. The experimental procedures for VGG16, DarkNet19 and ResNet18 models were replicated five times, maintaining the same parameter settings (e.g. batch size, epoch size) as employed in the proposed AlexNet model. Fig. 16 (a)-(e) provides a comprehensive comparison of different performance parameters, including accuracy, sensitivity, specificity, precision, and F1 score, for the four CNN models: AlexNet, VGG16, DarkNet19 and ResNet18.

As depicted in Fig. 16(a), the AlexNet model demonstrated the

highest accuracy compared to the VGG16, DarkNet19 and ResNet18 models for HC vs PD classification in dataset 1. The accuracy of the ResNet18 is slightly higher in dataset 2 compared to AlexNet, VGG16 and DarkNet19 for both HC vs PDSO and HC vs PDSF cases. This trend remained consistent across sensitivity, specificity, precision, and F1-score, as illustrated in Fig. 16 (b)-(e), respectively. In conclusion, even though the ResNet18 model shows slightly higher performance only for dataset 2, but AlexNet consistently exhibited superior performance compared to the other three models in both datasets. Therefore, we have decided that AlexNet is the best model for our proposed framework.

Additionally, we conducted a comparison between our proposed method and existing approaches for the same PD EEG datasets that we

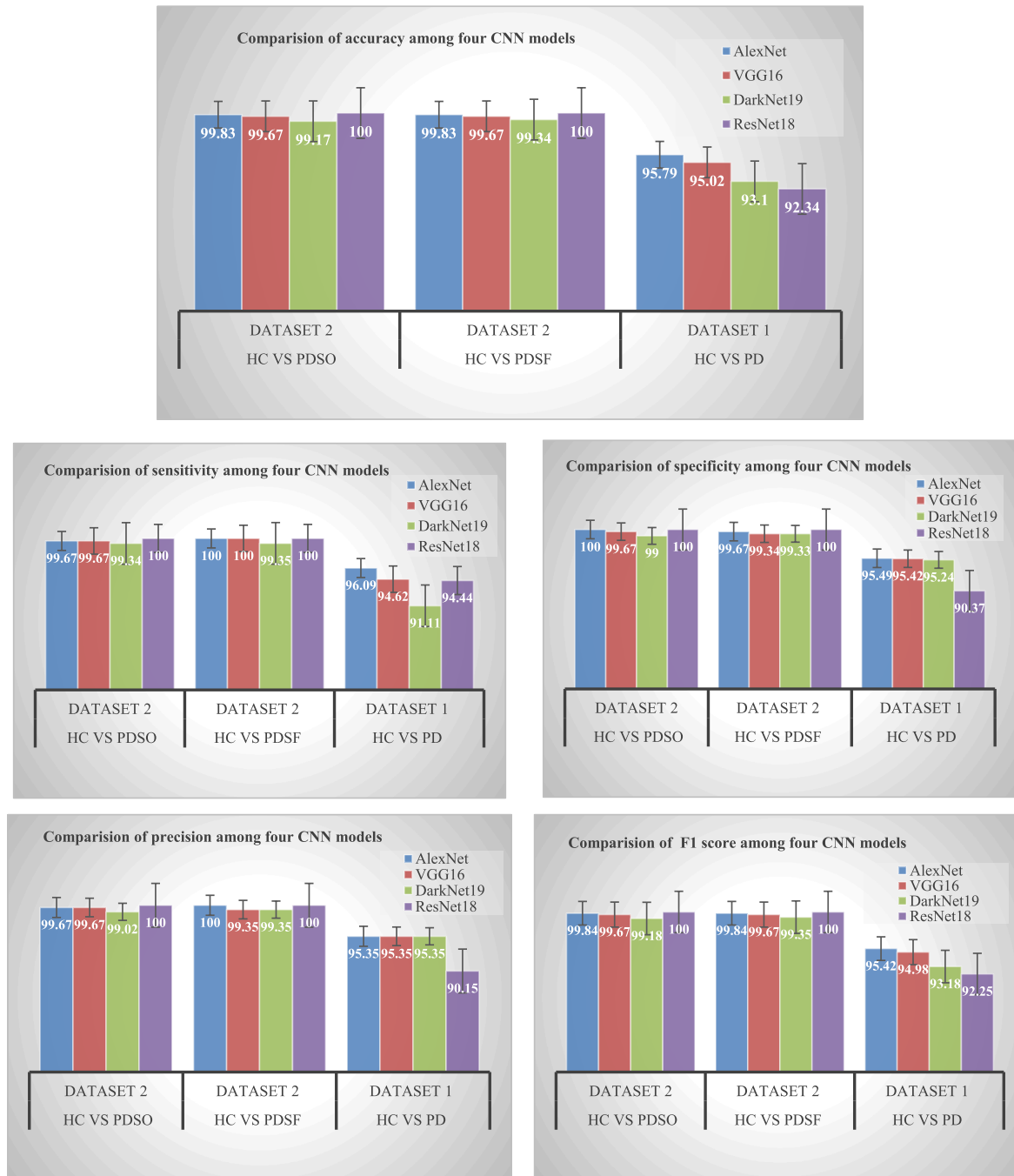


Fig. 16. Comparative analysis of performances among four CNN models within the proposed framework, (a) Accuracy comparison; (b) Sensitivity comparison; (c) Specificity comparison; (d) Precision comparison; (e) F1-score comparison.

**Table 8**

Comparison of the proposed scheme with state-of-the-art method for the same datasets.

Datasets	Authors	Methods	Classes	Overall Accuracy
Dataset 1: Iowa dataset:	Lee et al. [37]	Hjorth parameter and Gradient boosting decision tree + Gradient boosting decision tree	HC vs. PD	89.3%
	Anjum et al. [14]	Linear predictive coding + Hyperplanes	HC vs. PD	85.7%
	Sugden et al. [38]	a channel-wise convolutional neural network	HC vs. PD	83.8%
	Karaka & Latifo [2]	Gray-level co-occurrence matrix (GLCM) + SVM	HC vs. PD	85.71%
	Our proposed	SWT + Alexnet based CNN	HC vs. PD	95.79%
Dataset 2: UC San Diego	Qiu et al. [1]	Phase locking value and Power spectral density + Proposed MCNN	HC vs. PD_OFF	97.15%
	Khare et al. [12]	Tunable Q wavelet transform + Least square SVM	HC vs. PD_ON	98.27%
			HC vs. PD_OFF	96.13%
			HC vs. PD_ON	97.65%
	Aljalal et al. [39]	CSP + LogEn + SVM/KNN	Of-PD vs HC	99.41%
	Loh et al. [40]	Gabor transform, and 2D CNN	On-PD vs HC	95.76%
			HC vs PD without drug	99.44%
	Motin et al. [42]	With the optimal number + SVM (polynomial)	HC vs PD with medication	92.60%
			Of-PD versus HC	87.09%
			HC	
Aljalal et al. [41]	DWT + TShEn + KNN	On-PD vs HC	94.21%	
Our proposed	SWT + AlexNet based CNN	Of-PD vs HC	99.89%	
		HC vs PDSO	99.83%	
		HC vs PDSF	99.83%	

used in this study. Table 8 presents the latest findings on EEG-based PD detection, specifically focusing on the overall accuracy of various research works

conducted on two datasets: the Iowa dataset (dataset 1) and the UC San Diego dataset (dataset 2). Within the context of the Iowa dataset, which consists of 14 PD patients and 14 control subjects, several studies have been conducted on this dataset. The results depicted in Table 8 highlight the significant advancements achieved by our proposed model in terms of classification accuracy when compared to other relevant studies, such as Lee et al. [37], Anjum et al. [14], Sugden et al. [38], and Karaka & Latifo [2]. Our proposed model outperforms the other studies by a large margin. Specifically, it achieves an accuracy that is 11.99% higher than Sugden et al. [38], 10.09% higher than Anjum et al. [14], 10.08% higher than Karaka & Latifo [2], and 6.49% higher than Lee et al. [37].

The San Diego dataset, consisting of 15 PD patients and 16 controls, has been extensively studied by various researchers. The experiments conducted on this dataset include PD during ON medication (PDSO), OFF medication (PDSF), and healthy controls (HC). In Table 8, it is evident that our proposed method achieves the highest classification accuracy for PD during ON medication (PDSO). Additionally, for PD during OFF medication (PDSF) classification, our proposed model demonstrates nearly identical accuracy (99.83%) compared to the highest accuracy obtained by Aljalal et al. [41] (99.89%). These

results collectively demonstrate that the TFR based AlexNet CNN model we propose exhibits superior classification performance compared to parallel models when applied to the datasets utilized in this study. The superiority of our proposed model in EEG-based PD detection can be attributed to their deeper architecture, larger receptive fields,

utilization of fully connected layers, implementation of dropout regularization, and extensive research support.

## 5. Conclusion and future plans

The key objective of this study was to determine the brain region that provides vital information for efficient PD detection using EEG data and to improve the performance of the proposed method compared to existing approaches. To achieve this, a TFR-based AlexNet CNN framework was developed for EEG-based PD diagnosis. The WST effectively captured local and temporal properties of PD EEG data, while the AlexNet CNN model extracted complex features and detected spatial patterns at different scales, resulting in enhanced PD detection capabilities. The proposed framework's effectiveness was evaluated using two real datasets: Iowa dataset (dataset 1) and San Diego dataset (dataset 2). Through channel-wise analysis, the contribution of each EEG channel was assessed, leading to the identification of brain regions providing superior information for efficient PD diagnosis. Topographic maps, based on accuracy values of each channel, visually demonstrated the significance of AFz and AF4 channels, along with the frontal and central brain regions, in facilitating efficient PD detection.

The proposed model achieved impressive accuracy, sensitivity (SEN), specificity (SPE), positive predictive value (PPV), and F1 score for both datasets. On dataset 1, the model attained an accuracy of 95.79%, SEN of 96.09%, SPE of 95.49%, PPV of 95.35%, and F1 score of 95.42% for PD vs. HC classification. On dataset 2, the model achieved an accuracy of 99.84% for PDSF vs. HC classification, and also for PDSO vs. HC classification. The model also demonstrated excellent SEN, SPE, PPV, and F1 score of 100%, 99.67%, 100%, and 99.84%, respectively, for PDSF vs. HC classification, and 99.67%, 100%, 99.67%, and 99.84%, respectively, for PDSO vs. HC classification. These results highlighted the superiority of the TFR-based AlexNet CNN model over existing methods in effectively classifying PD-related EEG data. Furthermore, we evaluated the performance of the AlexNet model in comparison to three other CNN models, namely VGG16, DarkNet19 and ResNet18, within the proposed framework. The experimental results indicate that the AlexNet-based CNN exhibited superior performance in both datasets when compared to the other three CNN models. Based on the optimistic outcomes, the proposed model holds promising potential as a valuable and enduring aid for experts and clinicians in diagnosing PD. Additionally, the combination model can be extended to other medical signals, such as ECG, EOG, and EMG signals, suggesting potential applications and practical significance in various medical domains.

## CRedit authorship contribution statement

**Siuly Siuly:** Writing – review & editing, Writing – original draft, Methodology, Formal analysis, Data curation, Conceptualization. **Smith K. Khare:** Validation, Software, Formal analysis, Data curation. **Enamul Kabir:** Writing – review & editing, Validation, Investigation. **Muhammad Tariq Sadiq:** Visualization, Validation, Software, Investigation. **Hua Wang:** Validation, Supervision, Project administration, Investigation.

## Declaration of competing interest

The authors declare that they have no known competing financial interests or personal relationships that could have appeared to influence the work reported in this paper.

## References

- [1] L. Qiu, J. Li, J. Pan, Parkinson's disease detection based on multi-pattern analysis and multi-scale convolutional neural networks, *Front. Neurosci.* 16 (2022) 957181, <https://doi.org/10.3389/fnins.2022.957181>.

- [2] M.F. Karakaş, F. Latifoğlu, Distinguishing Parkinson's disease with GLCM features from the Hankelization of EEG signals, *Diagnostics* 13 (2023) 1769, <https://doi.org/10.3390/diagnostics13101769>.
- [3] Smith K. Khare, Varun Bajaj, U. Rajendra Acharya, PDCNNet: an automatic framework for the detection of Parkinson's disease using EEG signals, *IEEE Sensor. J.* 21 (15) (AUGUST 1, 2021).
- [4] World Health Organization. Parkinson Disease. Available online: Parkinson disease, World Health Organization (WHO), <https://www.who.int/news-room/fact-sheets/detail/parkinson-disease#:~:text=Global%20estimates%20in%202019%20showed,of%20over%20100%25%20since%202000..>
- [5] S. Selvaraj, S. Piramanayagam, Impact of gene mutation in the development of Parkinson's disease, *Genes Dis* 6 (2) (2019 Feb 27) 120–128, <https://doi.org/10.1016/j.gendis.2019.01.004>. PMID: 31193965; PMCID: PMC6545447.
- [6] A. Lee, R.M. Gilbert, Epidemiology of Parkinson disease, *Neurol. Clin.* 34 (4) (2016 Nov) 955–965, <https://doi.org/10.1016/j.ncl.2016.06.012>. Epub 2016 Aug 18. PMID: 27720003.
- [7] A. Reeve, E. Simcox, D. Turnbull, Ageing and Parkinson's disease: why is advancing age the biggest risk factor? *Ageing Res. Rev.* 14 (100) (2014 Mar) 19–30, <https://doi.org/10.1016/j.arr.2014.01.004>. Epub 2014 Feb 3. PMID: 24503004; PMCID: PMC3989046.
- [8] M.F. Beal, Mitochondria, oxidative damage, and inflammation in Parkinson's disease, *Ann. N. Y. Acad. Sci.* 991 (2003) 120–131.
- [9] Parkinson's Foundation. Parkinson's Statistics. Accessed on April 18, 2023, from <https://www.parkinson.org/Understanding-Parkinsons/Statistics>.
- [10] K. Li, B. Ao, X. Wu, Q. Wen, E. Ul Haq, J. Yin, Parkinson's disease detection and classification using EEG based on deep CNN-LSTM model, *Biotechnol. Genet. Eng. Rev.* 11 (2023 Apr) 1–20, <https://doi.org/10.1080/02648725.2023.2200333>. Epub ahead of print. PMID: 37039259.
- [11] P.D. Barua, S. Dogan, T. Tuncer, M. Baygin, U.R. Acharya, Novel automated PD detection system using aspirin pattern with EEG signals, *Comput. Biol. Med.* 137 (2021 Oct) 104841, <https://doi.org/10.1016/j.combiomed.2021.104841>. Epub 2021 Sep 6. PMID: 34509880.
- [12] Smith K. Khare, Varun Bajaj, U. Rajendra Acharya, Detection of Parkinson's disease using automated tunable Q wavelet transform technique with EEG signals, *Biocybern. Biomed. Eng.* 41 (2) (2021) 679–689, <https://doi.org/10.1016/j.bbe.2021.04.008>. ISSN 0208-5216.
- [13] A.P.S. De Oliveira, M.A. De Santana, M.A. Andrade, J.A.S. Gomes, M.T. Rodrigues, W.P.D. Santos, Early diagnosis of Parkinson's disease using EEG, machine learning and partial directed coherence, *Res. Biomed. Eng.* 36 (3) (2020) 311–331, <https://doi.org/10.1007/s42600-020-00072-w>.
- [14] F. Anjum, S. Dasgupta, R. Mudumbai, A.D. Singh, J.F. Cavanagh, N.S. Narayanan, Linear predictive coding distinguishes spectral EEG features of Parkinson's disease, *Park. Relat. Disord.* 79 (2020) 79–85, <https://doi.org/10.1016/j.parkrelidis.2020.08.001>.
- [15] R. Balestrino, A. Schapira, Parkinson disease, *Eur. J. Neurol.* 27 (1) (2019) 27–42, <https://doi.org/10.1111/ene.14108>.
- [16] R. Yuvaraj, U.R. Acharya, Y. Hagiwara, A novel Parkinson's disease diagnosis Index using higher-order spectra features in EEG signals, *Neural Comput. Appl.* 30 (4) (2018) 1225–1235, <https://doi.org/10.1007/s00521-016-2756-z>.
- [17] E. Naghsh, M.F. Sabahi, S. Beheshti, Spatial analysis of EEG signals for Parkinson's disease stage detection, *Signal, Image Video Proc.* 14 (2) (2020) 397–405, <https://doi.org/10.1007/s11760-019-01564-8>.
- [18] O. Faust, Y. Hagiwara, U. Raghavendra, R. Yuvaraj, N. Arunkumar, M. Murugappan, U.R. Acharya, A deep learning approach for Parkinson's disease diagnosis from EEG signals, *Neural Comput. Appl.* 32 (15) (2020) 10927–10933, <https://doi.org/10.1007/s00521-018-3689-5>.
- [19] M. Murugappan, W.B. Alshuaib, A.K. Bourisly, S.K. Khare, S. Sruthi, V. Bajaj, Tunable Q wavelet transform based emotion classification in Parkinson's disease using Electroencephalography, *PLoS One* 15 (11) (2020) e0242014, <https://doi.org/10.1371/journal.pone.0242014>.
- [20] N. Wagh, Y. Varatharajah, EEG-GCNN: augmenting Electroencephalogram-based neurological disease diagnosis using a domain-guided graph convolutional neural network, *Signal Process.* (2020). <http://arxiv.org/pdf/2011.12107.pdf>.
- [21] S. Xu, Z. Wang, J. Sun, Z. Zhang, Z. Wu, T. Yang, G. Xue, C. Cheng, Using a deep recurrent neural network with EEG signal to detect Parkinson's disease, *Ann. Transl. Med.* 8 (14) (2020) 874, <https://doi.org/10.21037/atm-20-5100>.
- [22] M. Koch, V.J. Geraedts, H. Wang, M.R. Tannemaat, T.G. Back, Automated machine learning for EEG-Based classification of Parkinson's disease patients, *Int. Conf. Big Data* (2019).
- [23] X. Shi, T. Wang, L. Wang, P. Liu, N. Yan, Hybrid convolutional recurrent neural networks outperform CNN and RNN in task-state EEG detection for Parkinson's disease, in: *Asia-Pacific Signal and Information Processing Association Annual Summit and Conference*, 2019, <https://doi.org/10.1109/apsipaasc47483.2019.9023190>.
- [24] S. Lee, R. Hussein, M.J. McKeown, A Deep convolutional-recurrent neural network architecture for Parkinson's disease EEG classification, in: *IEEE Global Conference on Signal and Information Processing*, 2019, <https://doi.org/10.1109/globalsip45357.2019.8969309>.
- [25] J. Hong, Y. Luo, M. Mou, J. Fu, Y. Zhang, W. Xue, T. Xie, L. Tao, Y. Lou, F. Zhu, Convolutional neural network-based annotation of bacterial type IV secretion system effectors with enhanced accuracy and reduced false discovery, *Briefings Bioinf.* 21 (5) (2020) 1825–1836, <https://doi.org/10.1093/bib/bbz120>. PMID: 31860715.
- [26] Zheng, et al., AnnoPRO: a strategy for protein function annotation based on multi-scale protein representation and a hybrid deep learning of dual-path encoding, *Genome Biol.* 25 (1) (2024) 41, 2024. PMID: 38303023.
- [27] Mou, et al., A transformer-based ensemble framework for the prediction of protein-protein interaction sites, *Research* 6 (2023) 240. PMID: 37771850.
- [28] Wang, et al., A task-specific encoding algorithm for RNAs and RNA-associated interactions based on convolutional autoencoder, *Nucleic Acids Res.* 51 (21) (2023) e110, 2023. PMID: 37889083.
- [29] J. Hong, Y. Luo, Y. Zhang, J. Ying, W. Xue, T. Xie, L. Tao, F. Zhu, Protein functional annotation of simultaneously improved stability, accuracy and false discovery rate achieved by a sequence-based deep learning, *Briefings Bioinf.* 21 (4) (2020 Jul 15) 1437–1447, <https://doi.org/10.1093/bib/bbz081>. PMID: 31504150.
- [30] Iowa dataset, The Iowa dataset analyzed for this study can be found in the following link: <https://bit.ly/3pP1pts..>
- [31] A.P. Rockhill, N. Jackson, J. George, A. Aron, N.C. Swann, Uc San Diego Resting state eeg data from patients with Parkinson's disease. California, CA, Tech. Rep. (2020).
- [32] H.W. Loh, C.P. Ooi, E. Palmer, P.D. Barua, S. Dogan, T. Tuncer, M. Baygin, U. R. Acharya, GaborPDNet: gabor transformation and deep neural network for Parkinson's disease detection using EEG signals, *Electronics* 10 (2021) 1740.
- [33] Z. Liu, G. Yao, Q. Zhang, J. Zhang, X. Zeng, Wavelet scattering transform for ECG beat classification, *Comput. Math. Methods Med.* 2020 (2020), <https://doi.org/10.1155/2020/3215681>. Article ID 3215681, 11 pages, 2020.
- [34] J. Anđén, S. Mallat, Multiscale scattering for audio classification, in: *International Society for Music Information Retrieval Conference*, 2011, pp. 657–662. Miami, Florida, USA.
- [35] Alex Krizhevsky, Ilya Sutskever, Geoffrey E. Hinton, ImageNet classification with deep convolutional neural networks, *Commun. ACM* 60 (6) (2017) 84–90, <https://doi.org/10.1145/3065386>.
- [36] Ahmet Esad Top, Hilal Kaya, Alexnet classification of EEG signals by using transfer learning on convolutional neural networks via spectrogram, in: *International Conference on Engineering Technologies (ICENTE18)*, 2018, pp. 156–161.
- [37] S.B. Lee, Y.J. Kim, S. Hwang, H. Son, S.K. Lee, K.I. Park, et al., Predicting Parkinson's disease using gradient boosting decision tree models with electroencephalography signals, *Parkinsonism Relat. Disorders* 95 (2022) 77–85, 10.1016/j.parkrelidis.2022.01.011.
- [38] R. Sugden, P. Diamandis, Generalizable electroencephalographic classification of Parkinson's Disease using deep learning, *medRxiv* (2022).
- [39] M. Aljalal, S.A. Aldosari, K. AlSharabi, A.M. Abdurraqeab, F.A. Alturki, Parkinson's disease detection from resting-state EEG signals using common spatial pattern, entropy, and machine learning techniques, *Diagnostics* 12 (5) (2022) 1033.
- [40] H.W. Loh, C.P. Ooi, E. Palmer, P.D. Barua, S. Dogan, T. Tuncer, et al., GaborPDNet: gabor transformation and deep neural network for Parkinson's disease detection using EEG signals, *Electronics* 10 (2021) 1740, <https://doi.org/10.3390/electronics10141740>.
- [41] M. Aljalal, S.A. Aldosari, M. Molinas, et al., Detection of Parkinson's disease from EEG signals using discrete wavelet transform, different entropy measures, and machine learning techniques, *Sci. Rep.* 12 (2022) 22547, <https://doi.org/10.1038/s41598-022-26644-7>.
- [42] M.A. Motin, M. Mahmud, D.J. Brown, Detecting Parkinson's disease from electroencephalogram signals: an explainable machine learning approach, in: *2022 IEEE 16th International Conference on Application of Information and Communication Technologies (AICT)*, Washington DC, DC, USA, 2022, pp. 1–6, <https://doi.org/10.1109/AICT55583.2022.10013589>.